Temperature-dependent magnetization and susceptibility of Fe_n/V_7 superlattices

M. Pärnaste,* M. van Kampen, R. Brucas, and B. Hjörvarsson
Department of Physics, Uppsala University, Box 530, 751 21 Uppsala, Sweden
(Received 3 September 2004; revised manuscript received 31 January 2005; published 31 March 2005)

We investigated the magnetic ordering of Fe_n/V_7 superlattices with Fe layer thicknesses in the range of $1.7 \leqslant n \leqslant 2.6$ monolayers. The temperature dependence of the magnetization and susceptibility was determined using the magneto-optical Kerr effect. The ordering temperature was found to vary almost linearly with the thickness of the Fe layers. Values for the critical exponent β were in the range 0.31–0.48, indicating three-dimensional behavior below T_C for all samples. A conclusive interpretation of the susceptibility data was hampered by tailing of $M(T)$ above T_C, resulting in a strong dependence on the excitation field. The temperature of the onset of an imaginary part of the susceptibility corresponded closely to the onset of (finite-size) magnetization. Since this temperature is not T_C, the onset of $\chi''(T)$ should not be used to directly determine the ordering temperature.

DOI: 10.1103/PhysRevB.71.104426 PACS number(s): 75.70.Cn, 75.40.Cx

I. INTRODUCTION

Most studies of dimensionality aspects of magnetic phase transitions have historically been performed on bulk systems. The influence of spatial dimensionality could be investigated by using layered magnetic compounds.[1] For example, the magnetic MnF_4 layers in Rb_2MnF_4[2] exhibit a strong intralayer coupling (J) and a weak interlayer coupling (J'), making the magnetic properties of this bulk compound two-dimensional-like. Modern growth techniques allow for the preparation of layered structures with an accuracy in the monolayer (ML) range. This opens completely different routes for the study of low-dimensional magnetism. For example, two-dimensional (2D) magnetism has been observed in few-ML thick films of, e.g., Fe on Ag,[3] on Pd[4] and on W.[5]

The effects of interlayer coupling can be investigated in ferromagnetic-nonmagnetic (FM-NM) multilayers.[6,7] The FM layers are coupled over the NM spacer layer by an RKKY-type of interaction,[8] which oscillates in both sign and magnitude with spacer layer thickness. The ML thickness control in preparing such multilayers gives a flexibility that is unequaled by the previously used bulk materials. In, for example, Fe/V superlattices, the inter- to intralayer coupling ratio can be varied in a wide range. Using published values for J[9] ($\approx$34 meV/atom) and J', a ratio $J'/J \approx 1/250$ can be estimated for a FM coupled Fe_2/V_5 superlattice ($J' \approx 125$ μeV/atom).[6] Choosing instead a 13 ML V spacer, corresponding to the maximum antiferromagnetic coupling, a ratio $J'/J \approx -1/1800$ is found ($J' \approx -19$ μeV/atom).[10] The above estimates were made using the bulk value for J. Since this is most likely an overestimation and a simplification[11] for a 2-ML film the actual ratios $|J'/J|$ will be higher.

For multilayers consisting of thin FM layers and having a weak interlayer coupling, i.e., $|J'/J| \ll 1$, a two-dimensional magnetic behavior is expected. However, close to T_C a transition to three-dimensional (3D) behavior may occur due to the divergence of the magnetic correlation length. Recently, Rüdt *et al.* reported 2D behavior in a FM coupled Fe_2/V_5 superlattice.[6,12] Fitting susceptibility data down to 10^{-4} in reduced temperature, a (two-dimensional) γ value of $\sim$1.72 was derived. Surprisingly, no crossover to 3D behavior was found. This observation was explained by a rapid decay of J' when approaching the ordering temperature.[6,13]

Here we will discuss the magnetic properties of a series of Fe/V superlattices in the FM-coupled region. This material combination is well characterized and can be grown with small roughness and high crystalline quality.[14] However, an intrinsic thickness variation originating from incomplete formation of a monolayer is always present in a non-phase-lock growth. This intrinsic imperfection might be of great importance when addressing the magnetic properties of this class of materials.

An Fe/V superlattice grown with an amount of Fe corresponding to an integer number (e.g., 2) of ML's is expected to be flatter and show less roughness than a layer grown with a deliberate deficit or surplus of Fe. Also, since 1 ML of Fe sandwiched between V layers is nonmagnetic,[15,16] an e.g., 1.7 ML sample will consist of ferromagnetic 2-ML thick islands coupled over weak, 1-ML thick links. One may therefore expect a reduction of the maximum correlation length for sub-2-ML samples, and also a percolation transition can occur at a certain thickness. Note that the magnitude of these effects depend strongly on the growth process, e.g., the amount of inter- and surface-diffusion during deposition.

The magnetic dimensionality is investigated by measuring the temperature dependence of the magnetization and the magnetic susceptibility. Close to T_C the magnetization can be described by a power law of the form

$$M = M_0(-t)^{\beta}, \tag{1}$$

where β is the critical exponent relating the magnetization to the reduced temperature, $t=(T-T_C)/T_C$. Similarly, the real part of the susceptibility can be described by a power law of the form

$$\chi' \propto t^{-\gamma}, \tag{2}$$

with γ the critical exponent of the susceptibility. The critical exponents take on discrete values, depending on the mag-

 ©2005 The American Physical Society

netic dimensionality or the universality class of the system. For example, the 2D Ising system is exactly solvable yielding $\beta=0.125$ and $\gamma=1.75$. Bramwell and Holdsworth determined β to be ~ 0.23 for the 2D XY model[17] and for 3D models β varies between 0.31 and 0.35 and γ between 1.25 and 1.38, depending on the spin dimensionality of the model.

Here we will discuss the influence of the thickness of the Fe layer on the magnetic behavior, e.g., the impact on the critical exponents β and γ and the presence or absence of a dimensionality crossover[2,18] close to the ordering temperature. As the thickness of the V layers is fixed at 7 ML, the inter- to intralayer coupling ratio J'/J can be assumed constant throughout the sample series. Lacking experimental means to deduce J' for ferromagnetically coupled multilayers, but with the knowledge that J' crosses zero at approximately 10 ML of V[19] and that $J'/J \approx 1/250$ for 5 ML of V,[12] we estimate J'/J to be $\approx 1/400$.

It is of interest to see if the absence of dimensionality crossover previously reported[6,12] is a result of the smoothness of the magnetic layers and, if so, whether a deliberate fractional roughness in the magnetic layers can induce a dimensionality crossover.

II. SAMPLE PREPARATION AND EXPERIMENTAL DETAILS

A. Sample preparation

The Fe_n/V_7 superlattices with different Fe layer thicknesses were grown on polished MgO(001) $10\times10\times0.5$ mm^3 single-crystal substrates by dc magnetron sputtering from separate Fe (99.95%) and V (99.95%) targets arranged in a cluster geometry. The MgO(001) substrates were introduced into the growth chamber and outgassed at about 700 °C for 1 h under ultrahigh-vacuum conditions before deposition. A growth temperature of 330 °C for the Fe/V superlattices was chosen according to previous growth optimization.[14] The background pressure was around 5×10^{-10} Torr and an argon (99.99%) gas flow was kept at a partial pressure of 2.5×10^{-3} Torr during deposition. The bilayer sequence was repeated 50 times starting and ending each sample with a V layer. After deposition of the V and Fe layers, the samples were cooled down to room temperature and capped with a 3 nm thick amorphous Al_2O_3 layer to prevent oxidation of the top V layer. The deposition rate of Fe was kept low at 0.04 Å/s to ensure a precise thickness control of the Fe layer. The deposition rates for the V and Al_2O_3 layers were 0.45 and 0.06 Å/s, respectively. These values were obtained from thickness calibration measurements using x-ray reflectivity analysis.

A series of ten samples was grown, increasing the targeted Fe thickness with 0.15 Å (0.1 ML) between samples. Low- and high-angle x-ray measurements were used to characterize the samples. Figure 1 shows low-angle scans for all samples in the series, full scans are shown for the 1.7, 2.2, and 2.6 ML samples, while only the peak regions are displayed for the remaining samples. The Kiessig fringes, extending up to $\sim 7°$, are indicative of a well-defined total thickness. The crystalline quality was confirmed by the narrow widths of rocking curves at the high-angle Bragg peak ($\leqslant 0.1°$). The determined Fe thicknesses are summarized in Table I, showing the excellent growth control by a $\leqslant 0.05$ ML difference between real and targeted Fe thickness (except for the 2.5 ML sample).

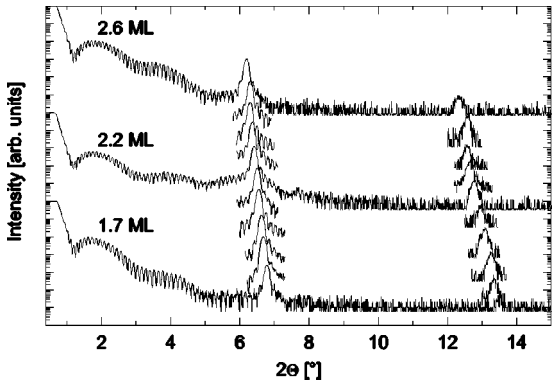

FIG. 1. Low-angle x-ray reflectivity for all samples in the series. The scans are offset from each other for clarity. Note the well-developed Kiessig fringes extending up to $\sim 7°$.

B. Experimental details

The temperature dependence of the susceptibility and the magnetization was studied using a magneto-optic technique. The samples are placed in an optical cryostat (2.2–500 K), allowing wide-angle optical access. In-plane fields up to 2 mT can be applied using a pair of Helmholtz coils outside the cryostat. The whole system is shielded by three separate layers of mu-metal to achieve low ($\leqslant 1$ μT) stray fields at the sample position. The axial stray field can be reduced further to below 0.1 μT by sending a dc current through the Helmholtz coils. Active compensation of the remaining stray fields did not significantly affect the results and was, therefore, not used.

TABLE I. Thicknesses obtained from x-ray measurements. The V thickness is fixed at 7 ML (10.60 Å). Using the bulk lattice parameter of Fe to convert to MLs, the difference between the real and intended thickness is $\leqslant 0.05$ ML (except for the 2.5 ML sample).

Intended Fe thickness (ML)	Bilayer thickness (Å)	Obtained Fe thickness (ML)
1.7	13.02	1.69
1.8	13.22	1.84
1.9	13.32	1.90
2.0	13.48	2.01
2.1	13.57	2.07
2.2	13.76	2.21
2.3	13.89	2.30
2.4	14.03	2.39
2.5	14.00	2.37
2.6	14.25	2.55

The magnetic response of the sample is detected by the Kerr rotation of the reflected laser light, using a crossed-polarizer configuration to convert the small polarization changes to an intensity variation. For the ac-susceptibility measurements, a small (2.8 μT) oscillatory field with a frequency of 213 Hz is applied. No frequency dependence was observed on lowering the frequency to about 20 Hz, confirming the quasistatic nature of the experiment. The spatial variation of the excitation field over the sample is below 1%. Using a lock-in technique, the detector signal is analyzed phase sensitively, allowing the extraction of both the real (χ') and the imaginary (χ'') parts of the susceptibility. The temperature dependence of the magnetization is derived from magnetization loops measured with the same setup. The loops are obtained by applying a ~7 Hz oscillating field to the sample and simultaneously recording the detector signal and the applied field in time. By phase-sensitive averaging of a number of cycles, low-noise magnetization loops can be obtained in approximately 20 s, even at T_C. No significant effect of the frequency on the shape of the loops could be detected for frequencies between 0.1 and 10 Hz.

The 630 nm laser light used in our magneto-optical setup has a penetration depth of ~200 Å. Therefore, only the top ~30% of the ~700 Å thick samples is probed. From previous growth studies on Fe/V it is known that the layer quality does vary with thickness.[14] However, most defects are formed close to the substrate, while successive bilayers are of nearly constant quality.

During the measurements the temperature is ramped up and down in a region around T_C at rates less than 50 mK/min to ensure thermal equilibrium in the sample. The sample is clamped to a Cu sample holder surrounded by a thermal radiation shield ensuring good thermal contact. The actual sample temperature is measured using a resistive temperature sensor placed close to the sample. The precision of the temperature reading was confirmed by the lack of hysteresis in the magneto-optic signal for increasing and decreasing temperatures.

III. RESULTS AND DISCUSSION

To extract the critical exponents β and γ, the temperature dependence of the magnetization and susceptibility was measured for all samples. Figure 2 shows the remanent magnetization of a representative sample, as determined from a series of magnetization loops. A fitting of the data with Eq. (1) in the region 79–84 K yields a T_C of 84.9±0.1 K and a β of 0.34±0.01. We found that for all samples T_C is relatively insensitive to the fitting interval used. T_C and β were also determined by a method proposed by Kouvel and Fisher[20,21]

$$\frac{M}{dM/dT} = \frac{T - T_C}{\beta}. \tag{3}$$

By plotting $M/(dM/dT)$ versus T one obtains a straight line with slope $1/\beta$ and the intersect with the horizontal axis gives T_C. The inset of Fig. 2 shows $M/(dM/dT)$ plotted as a function of temperature. Fitting the data in the linear region

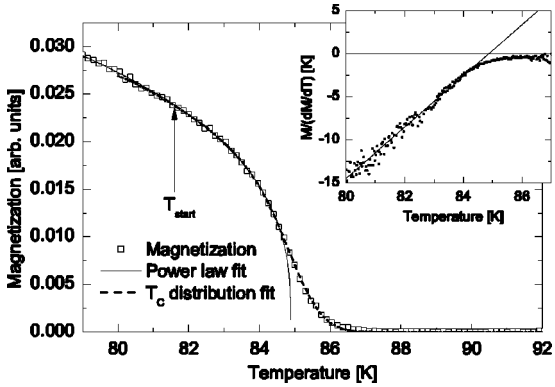

FIG. 2. Magnetization versus temperature for the sample with 2.3 ML of Fe. The full line is a fit using Eq. (1), resulting in T_C = 84.9±0.1 K and β=0.34±0.01. The dashed line is a fit using a distribution of T_C's, yielding T_C=84.9±0.3 K and β=0.34±0.02. T_{start}=0.95 T_C marks the start of the fitted region. The inset shows $M/(dM/dT)$ vs T, where the straight line is a linear fit with slope $1/\beta$ (β=0.337±0.007) where the x-axis intercept marks T_C (T_C =84.9±1 K).

of $M/(dM/dT)$, similar values for T_C and β (84.9±1 K and 0.337±0.007, respectively) are obtained.

All measured $M(T)$ curves show finite-size tailing. Inhomogeneities in the sample can result in finite-sized regions with slightly different T_C, causing a broadening of the transition and thereby a tail to $M(T)$. The inhomogeneities will also put an upper limit on the divergence of the correlation length. This results in a second type of finite-size tailing often encountered in numerical simulations,[22] and possibly also in experiments.[4,23,24] One way to deal with the tailing of $M(T)$ is by assuming a (Gaussian) distribution of T_C's. This method has, for example, been used to describe the magnetization of ML thick Fe films deposited on W.[25] Fitting magnetization data down to T=0.95 T_C with a power-law decay convoluted with a Gaussian distribution of critical temperatures we find T_C=85.9±0.1 K and β=0.34±0.09, cf. the dashed line in Fig. 2.

In Fig. 3 the remanent magnetization of all samples is compared. The magnetization is plotted as a function of re-

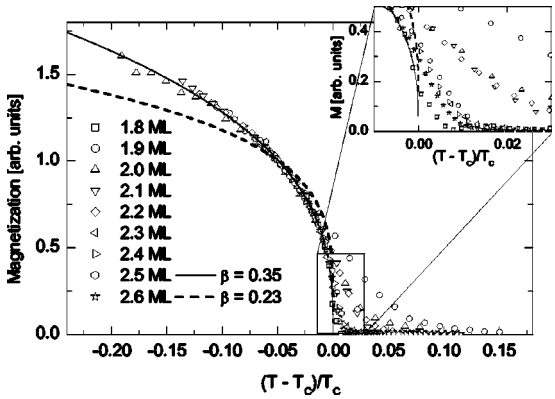

FIG. 3. Normalized M vs reduced temperature for all samples in the series. The magnetization curves are normalized at t=−0.05. The full and dashed lines are plots of Eq. (1) with β=0.35 and 0.23, i.e., the 3D Heisenberg model and 2D XY model, respectively.

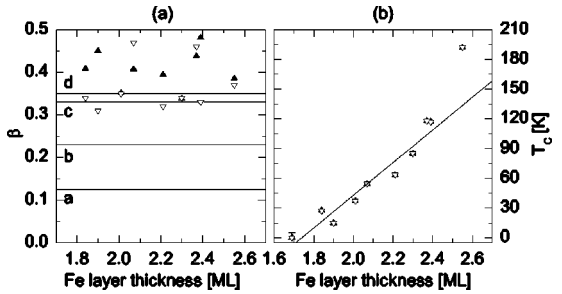

FIG. 4. Results of power law fitting of $M(T)$ data. Closed triangles represent a direct fit, open triangles represent results assuming a Gaussian distribution of critical temperatures. (a) Obtained values of β vs Fe thickness. The horizontal lines represent the β values of the a. 2D Ising, b. 2D *XY*, c. 3D Ising, and d. 3D Heisenberg models. (b) Obtained values of T_C vs Fe thickness, the solid line serves as a guide to the eye.

duced temperature and is normalized to 1 at $t=-0.05$. The data should therefore collapse on a single curve when belonging to the same universality class. Apart from finite-size differences close to the ordering temperature, all curves show the same functional behavior. The full and dashed lines in Fig. 3 represent Eq. (1) for, respectively, $\beta=0.35$ (3D Heisenberg) and $\beta=0.23$ (2D *XY*), showing a far better correspondence with the former.

Directly fitting the individual curves with the power law of Eq. (1) yields β values in the range 0.34–0.48, cf. Fig. 4(a) (closed triangles). Using a T_C distribution, β values between 0.31 and 0.47 are obtained (open triangles). No correlation between the β values and the Fe thicknesses is found for any of the fitting methods used. On the other hand, the T_C's obtained from fitting the $M(T)$ curves with Eq. (1) [Fig. 4(b), closed triangles] and using a T_C distribution (open triangles) show an almost monotonic increase of T_C with the Fe thickness. This confirms the accurate control of the Fe thickness in the different samples. No ferromagnetism was observed for the sample with 1.7 ML of Fe down to a temperature of 5 K. In summary, the magnetization data show three-dimensional critical exponents for all samples and an almost linear increase of T_C with the Fe layer thickness.

Apart from the magnetization, also the magnetic susceptibility has been measured for all samples in the series. Figure 5 shows the temperature dependence of the real part of the susceptibility for two samples having Fe thicknesses of 2.0 and 2.6 ML. As is seen in the figure, both peak position and width vary between samples. The inset of Fig. 5 shows the relation between the full width at half maximum (FWHM) of χ' and the tailing of $M(T)$, the latter expressed as the standard deviation of the Gaussian T_C distribution σ_{T_C}. Note that all values are reported as reduced temperatures using T_C's derived from the magnetization data.

In Fig. 6 the real and imaginary part of the susceptibility of the sample with 2.3 ML of Fe is shown, measured using two different excitation amplitudes (2.8 and 14 μT). The dashed vertical line marks T_C as determined from $M(T)$ (see, e.g., Fig. 2). Despite the small excitation amplitudes used, a clear excitation field dependence is observed. The differences occur even above T_C, e.g., the peak in χ' shifts from

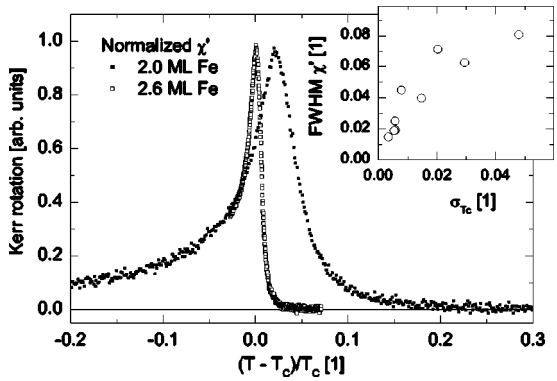

FIG. 5. Normalized susceptibility for two samples with 2.0 and 2.6 ML of Fe, measured using an excitation amplitude of 2.8 μT. The inset shows the relation between the FWHM of $\chi'(T)$ and the standard deviation of the Gaussian T_C distribution (both in reduced temperature).

$T>T_C$ to $T<T_C$ on increasing the excitation amplitude. Also this effect is related to $M(T)$ tailing in combination with the very low coercivity of the investigated samples. Figure 7 shows the coercivity H_C of the 2.3 ML sample versus temperature, as determined from magnetization loops. The dashed horizontal lines represent the excitation amplitudes used in the susceptibility experiments. The figure shows that for the lowest (2.8 μT) excitation ferromagnetic switching will contribute to the susceptibility signal[26] for $85.5 \lesssim T \lesssim 87$ K, where the upper bound is the approximate maximum temperature at which a finite $M(T)$ is observed (cf. Fig. 2). For the samples studied, having almost square hysteresis loops, the effect is severe and will manifest as a shifting of the susceptibility peak toward lower temperatures when the excitation field is increased and subsequently the lower temperature bound is decreased. Indeed, χ' peaks very close to 85.5 K for the 2.8 μT excitation, while the susceptibility measured with the higher field of 14 μT continues to increase even below T_C. What appears to be a similar shift is seen in susceptibility data of Elmers *et al.*[25] The same effect is also responsible for the variation in peak position between

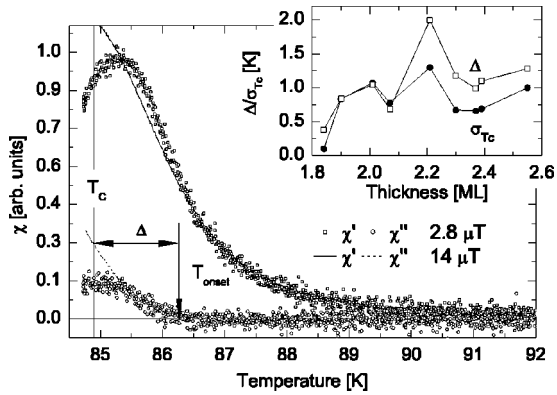

FIG. 6. Real (χ') and imaginary (χ'') parts of the susceptibility for two different excitation amplitudes, 2.8 and 14 μT. The vertical line shows the position of T_C as determined from power-law fitting of magnetization data. The arrow indicates the onset of χ'', Δ is its difference with respect to T_C. Inset: Δ and σ_{T_C} vs Fe thickness.

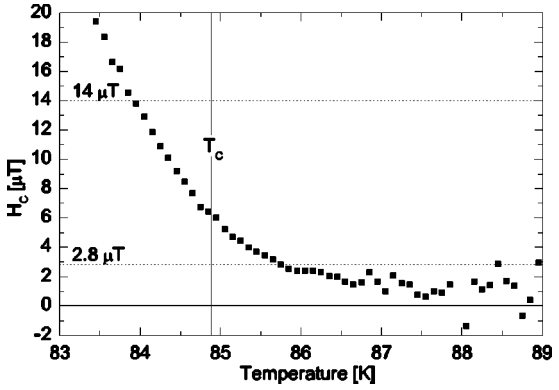

FIG. 7. Coercive field vs temperature for the sample with 2.3 ML of Fe. The horizontal dotted lines mark the values of the applied fields used in our measurements (2.8 and 14 μT, respectively). The vertical line marks T_C as determined from magnetization data.

samples (cf. Fig. 5), which is strongly dependent on the coercivity.

A conclusive analysis of susceptibility data is complex, as a number of factors cause deviations from Eq. (2). For example, χ generally does not diverge nor peak at T_C due to, for example, a finite demagnetization factor, imperfections that limit the divergence of the correlation length and domain wall movements below T_C.[27,28] Also, when measuring only the susceptibility, T_C has to be estimated from $\chi(T)$. Different empirical methods exist to deal with these issues, e.g., excluding data close to T_C, assuming T_C at the peak[29,30] or at a second peak or "hump"[31] in the susceptibility data or by fitting several parameters including T_C.[32]

In the paper by Rüdt *et al.*, showing 2D behavior in an Fe_2/V_5 multilayer, a different approach is taken. T_C is chosen at the onset of the imaginary part of the susceptibility, χ'', a temperature noted to correspond to the onset of finite remanence as determined from magnetization loops. Only the effect of the demagnetization factor N is considered and corrected for. Assuming that χ diverges at T_C, N can be determined from the measured susceptibility χ_{meas}. The true internal susceptibility χ_{int} can then be derived from the following relation:[33]

$$\chi_{\text{int}}^{-1} = \chi_{\text{meas}}^{-1} - N. \tag{4}$$

We see some problems with the foregoing analysis. First of all there are problems with respect to the determination of T_C. From our measurements of $M(T)$ and $\chi(T)$ on similar samples, we find that T_C is always considerably lower than the temperature at the onset of χ'', T_{onset}. In the inset to Fig. 6, the difference $\Delta = T_{\text{onset}} - T_C$ is plotted as a function of Fe thickness (open squares). Also shown is σ_{T_C} (closed circles), a measure of the finite-size tailing to $M(T)$. The strong correlation between Δ and σ_{T_C} shows that T_{onset} indicates the onset of hysteretic losses and a finite magnetization, rather than T_C. Only for samples with a negligible tailing will T_{onset} correspond to T_C.

Second, by using Eq. (4) one assumes that the only limiting factor to the divergence of χ is a finite demagnetization factor. However, finite-size effects will also limit the divergence of the correlation length and therefore χ, invalidating this simple analysis. Moreover, it is questionable whether one can experimentally determine χ at T_C using a finite field excitation. Due to the finite magnitude of the excitation and the saturation of $M(H)$, $\chi_{\text{meas}}(T_C)$ will inherently not diverge. Also, any finite-size tailing to $M(T)$ will affect $\chi(T_C)$ by contributions from ferromagnetic switching.

Analysis of $\chi(T)$ using T_C's determined from $M(H,T)$ data, fitting the data to Eq. (2) and above the tailing-affected regime, e.g., from $t \approx 2 \times 10^{-2}$ to $t \approx 1 \times 10^{-1}$, yields poor fits and γ values in the range 1.7–3.4. It is apparent that no generalized conclusions about dimensionality can be drawn from these results.

The changes in remanent magnetization with temperature are consistent with 3D fluctuations below the ordering temperature. Therefore, the transitions must be regarded as 3D when $T \leqslant T_C$. Due to the excitation field dependence of the susceptibility and the resulting uncertainties, we cannot determine the dimensionality of the fluctuations above T_C. Hence, no general conclusions can be drawn on a dimensionality crossover for this particular set of samples.

IV. CONCLUSIONS

We have studied the magnetic properties of Fe/V superlattices as function of the thickness of the magnetic Fe layers with intermediate interlayer coupling. The critical temperature T_C showed almost linear and close to monotonic increase with increasing Fe layer thickness, consistent with a high level of control of the growth parameters. Directly fitting a power-law decay to the $M(T)$ data yielded critical exponents β in the range 0.34–0.48. Fits assuming a Gaussian distribution of T_C resulted in β values in the range 0.31–0.47.

No clear trend in β as a function of the fractional thickness of the Fe layers was observed. However, the correspondence between our data and the power-law decay with $\beta = 0.35$ is obvious. We thus conclude 3D magnetic interactions and fluctuations below the ordering temperature for all samples in this series. The observed 3D nature of the fluctuations indicate that J' is not negligible with respect to J, possibly due to a much weaker intralayer interaction in the few-ML thick Fe sheets.

The analysis of the susceptibility data proves difficult. The magnetization shows a very low coercivity and a ferromagnetic component extending above T_C. Therefore, ferromagnetic switching contributes to $\chi(T)$ even at the lowest excitation fields used. A power-law fitting of the susceptibility data outside the ferromagnetic region yielded poor fits and γ values in the range 1.7–3.4, not allowing for a conclusive statement on the dimensionality above T_C.

We believe that for a proper interpretation of susceptibility data, knowledge of $M(H,T)$ is crucial. The susceptibility data alone contains no clear markers of T_C, e.g., neither the peak in χ' nor the onset of a finite χ'' corresponds to T_C. Finding T_C by extended curve fitting is mainly based on the

belief that $\chi(T)$ is over a large range best described by the (approximate) power law. Also, the effects of tailing could not have been inferred from the susceptibility data alone. Although a relation between the peak width and the tailing to $M(T)$ was found, the width will depend on other sample specific factors as, for example, coercivity and domain wall mobility. Hence, the relation between peak width and tailing is only relevant in comparing samples of the same type.

ACKNOWLEDGMENTS

The authors wish to thank Professor S. T. Bramwell for fruitful discussions. This work was carried out with financial support from the Swedish Foundation for Strategic Research, the Swedish Research Council, and the Göran Gustafsson foundation.

*Electronic address: martin.parnaste@fysik.uu.se

[1] L. J. de Jongh and A. R. Miedema, Adv. Phys. **23**, 1 (1974).
[2] *Magnetic Properties of Layered Transition Metal Compounds*, edited by L. J. de Jongh (Kluwer Academic Publishers, Dordrecht, 1990).
[3] Z. Q. Qiu, J. Pearson, and S. D. Bader, Phys. Rev. Lett. **67**, 1646 (1991).
[4] C. Liu and S. D. Bader, J. Appl. Phys. **67**, 5758 (1990).
[5] H. J. Elmers, J. Hauschild, and U. Gradmann, J. Magn. Magn. Mater. **140-144**, 1559 (1995).
[6] C. Rüdt, P. Poulopoulos, J. Lindner, A. Scherz, H. Wende, K. Baberschke, P. Blomquist, and R. Wäppling, Phys. Rev. B **65**, 220404 (2002).
[7] U. Bovensiepen, F. Wilhelm, P. Srivastava, P. Poulopoulos, M. Farle, A. Ney, and K. Baberschke, Phys. Rev. Lett. **81**, 2368 (1998).
[8] M. A. Ruderman and C. Kittel, Phys. Rev. **96**, 99 (1954).
[9] C. Kittel, *Introduction to Solid State Physics*, 7th ed. (Wiley, New York, 1996).
[10] V. Leiner, K. Westerholt, A. M. Blixt, H. Zabel, and B. Hjörvarsson, Phys. Rev. Lett. **91**, 037202 (2003).
[11] S. S. A. Razee, J. B. Staunton, L. Szunyogh, and B. L. Gyorffy, Phys. Rev. Lett. **88**, 147201 (2002).
[12] C. Rüdt, P. Poulopoulos, K. Baberscke, P. Blomquist, and R. Wäppling, Phys. Status Solidi A **189**, 363 (2002).
[13] J. Lindner, C. Rüdt, E. Kosubek, P. Poulopoulos, K. Baberschke, P. Blomquist, R. Wäppling, and D. L. Mills, Phys. Rev. Lett. **88**, 167206 (2002).
[14] P. Isberg, B. Hjörvarsson, R. Wäppling, E. B. Svedberg, and L. Hultman, Vacuum **48**, 483 (1997).
[15] D. Labergerie, K. Westerholt, H. Zabel, and B. Hjörvarsson, J. Magn. Magn. Mater. **225**, 373 (2001).
[16] S. Mirbt, I. A. Abrikosov, B. Johansson, and H. L. Skriver, Phys. Rev. B **55**, 67 (1997).
[17] S. T. Bramwell and P. C. W. Holdsworth, J. Phys.: Condens. Matter **5**, L53 (1993).
[18] R. J. Birgeneau, Phys. Rev. B **41**, 2514 (1990).
[19] B. Hjörvarsson, J. A. Dura, P. Isberg, T. Watanabe, T. J. Udovic, G. Andersson, and C. F. Majkrzak, Phys. Rev. Lett. **79**, 901 (1997).
[20] J. S. Kouvel and M. E. Fisher, Phys. Rev. **136**, 1626 (1964).
[21] S. N. Kaul, Phys. Rev. B **23**, 1205 (1981).
[22] J. M. Yeomans, *Statistical Mechanics of Phase Transitions* (Oxford, London, 1992).
[23] P. Schilbe and K. H. Rieder, Europhys. Lett. **41**, 219 (1998).
[24] W. Dürr, M. Taborelli, O. Paul, R. Germar, W. Gudat, D. Pescia, and M. Landolt, Phys. Rev. Lett. **62**, 206 (1989).
[25] H. J. Elmers, J. Hauschild, and U. Gradmann, Phys. Rev. B **54**, 15 224 (1996).
[26] A. Aspelmeier, M. Tischer, M. Farle, M. Russo, K. Baberschke, and D. Arvantis, J. Magn. Magn. Mater. **146**, 256 (1995).
[27] C. S. Arnold, M. Dunlavy, and D. Venus, Rev. Sci. Instrum. **68**, 4212 (1997).
[28] X. C. Kou, R. Grössinger, G. Hilscher, H. R. Kirchmayr, and F. R. de Boer, Phys. Rev. B **54**, 6421 (1996).
[29] U. Stetter, M. Farle, K. Baberschke, and W. G. Clark, Phys. Rev. B **45**, 503 (1992).
[30] G. Garreau, M. Farle, E. Beaurepaire, and K. Baberschke, Phys. Rev. B **55**, 330 (1997).
[31] U. Bovensiepen, C. Rüdt, P. Poulopoulos, and K. Baberschke, J. Magn. Magn. Mater. **231**, 65 (2001).
[32] M. J. Dunlavy and D. Venus, Phys. Rev. B **69**, 094411 (2004).
[33] D. Jiles, *Introduction to Magnetism and Magnetic Materials*, 2nd ed. (Chapman and Hall, London, 1998).